Available online at www.sciencedirect.com
SCIENCE DIRECT
Polymer 47 (2006) 1436–1442
polymer
www.elsevier.com/locate/polymer

# Homology modeling and molecular dynamics studies on the tomato methyl jasmonate esterase

Wei-Wei Han, Ze-Sheng Li *, Qing-Chuan Zheng, Chia-chung Sun

*State Key Laboratory of Theoretical and Computational Chemistry, Institute of Theoretical Chemistry, Jilin University, Changchun 130023, People's Republic of China*

Received 5 October 2005; received in revised form 22 November 2005; accepted 22 November 2005
Available online 18 January 2006

**Abstract**

Jasmonic acid (JA) is a plant volatile that acts as an important cellular regulator mediating diverse developmental processes and defense responses. Not only the attacked plant but also neighboring plants are affected, becoming more attractive to herbivore predators and less susceptible to invaders. The three-dimensional (3D) model of methyl jasmonate esterase (MJE), which is only responsible for methyl jasmonate (MeJA)-cleaving activity, is constructed based on the crystal structure of salicylic acid-binding protein 2 (SABP2, PDB code 1XKL) by using InsightII/Homology module, and further refined using unrestrained dynamics simulations. With the aid of understanding the molecular interactions between the natural substrate: MeJA and MJE, a 3D model of the complex MeJA–MJE is developed by molecular docking program, and the result may be helpful to explain the experimental realization and the new mutant designs as well. The results indicate that the general 3D organization of MJE is a typical α/β hydrolase superfamily and comprises a central, parallel or mixes β sheet surrounded by α helices. The catalytic residues always constitute a highly conserved triad: Ser83, Asp211, His240, which is consistent with experimental observation. In addition, the key binding-site residues of Thr107 and Leu214 play an important role in the catalysis of MJE. One important finding is that the identification of the key binding site residues of Ser83, which plays an important role in the catalysis of MJE and this is in consistent with experimental observation. The inhibitor phenylmethanesulfonyl fluoride is docked to MJE. Our results also show that His240 and His82 are important in inhibition and it may be helpful for the future inhibitor study.


*Keywords:* Methyl jasmonate esterase; Molecular dynamics; Docking

## 1. Introduction

Jasmonates are important in intracellular regulators mediating diverse developmental processes, such as seed germination, flower and fruit development, leaf abscission, and senescence [1–4]. In addition, jasmonates induce plant defense responses against a group of pathogens and mechanical or herbivorous insect-driven wounding [5]. In particular, methyl jasmonate (MeJA) has become a strong candidate for airborne signals that mediate interplant communication for defense responses [6]. They have hormone properties, help regulating plant growth and development and they seem to participate in leaf senescence and in the defense mechanism against fungi [7]. Just like all other plant hormones, jasmonates have both activating and inhibiting effects [8,9]. Synergistic and antagonistic effects on other hormones have been observed, too. Jasmonate derivatives induce the accumulation of so-called jasmonate-induced proteins that were found in all plant species tested. Their accumulation can also be caused by desiccation or abscisic acid (ABA) effects [10]. Jasmonates not only regulate the transcription of these proteins, but also influence the rate of translation of different groups of mRNA [11]. They do, for example, decrease the production rate of several essential housekeeping proteins. Recent analysis reveals that MeJA must be demethylated prior to becoming active and thus root growth inhibition is mediated by MeJA through JA [1,12]. However, if MeJA is considered to be a signal, there must be a way to regulate the signal by controlled formation and perhaps more important by its controlled inactivation [1]. A candidate for performing the latter task is an esterase, previously characterized in tomato. In tomato cell cultures, only one MeJA-hydrolysing enzyme can be identified by activity-guided protein purification, named methyl jasmonate esterase (MJE). Moreover, it could be assumed that MJE is

* Corresponding author. Tel.: +86 431 849 8960; fax: +86 431 894 5942.
*E-mail address:* zeshengli@mail.edu.cn (Z.-S. Li).

0032-3861/$ - see front matter © 2005 Elsevier Ltd. All rights reserved.
doi:10.1016/j.polymer.2005.11.092

a member of α/β-hydrolase fold proteins. As further support of this assumption, MJE could be irreversibly inhibited by phenylmethanesulfonyl fluoride [13].

To our best knowledge, the 3D structure of MJE is not known. In the present paper, the 3D model of MJE is obtained by using homology modeling program based on the known structure of tomato SABP2 (PDB code 1XKL) [14], and then the 3D model of MJE is used to search the active site and carry out the binding studies by flexible docking with the ligands (substrate and inhibitor). Our results may be helpful for further experimental studies for this α/β hydrolase superfamily.

## 2. Theory and methods

All simulations are performed on the SGI O3800 workstations by using InsightII software package developed by Biosym Technologies [15]. The sequence of MJE is obtained from the databank in the National Center for Biotechnology Information (www.ncbi.nlm.nih.gov). In the molecular mechanical and dynamical calculations, the consistent-valence force field (CVFF) is employed.

### 2.1. 3D Model building

The homology module is used to build the initial MJE model [16]. The homology is searched by BLAST program [17]. The high sequence identity between MJE and SABP2 is 45% as shown in Fig. 1. The first requirement in the construction of MJE model is a multiple sequence alignment among these templates. The sequence alignment is based on identifying structurally conserved regions (SCR) common to the three templates. A high level of sequence identity should guarantee more accurate alignment between the target sequences. The second step is to generate a multiple sequence alignment of MJE with three templates. An initial 3D structure of MJE is obtained by transferring the backbone coordinates of SABP2 residues to the corresponding target protein, except for several variable regions (LOOPs) as indicated in Fig. 1. In order to construct the structural variable regions a loop-searching algorithm over the databank of known crystal structure is used. The residues at the N-terminus and C-terminus are generated through end-repair by using InsightII/Homology program. For the remaining side chains, library values of rotamers are adopted. Through the procedure mentioned above, an initial model is completed. All sequences are imported into the ClustalW program (version 1.83).

The initial model is improved by energy minimization. After 200 steps of conjugate gradient (CG) minimization performed, the MD simulation is carried out to check the quality of the model structures by testing their stability via performing 350 ps simulations at a constant temperature 298 K. Explicit solvent model TIP3P water is used with a 10 Å water cap from the center of mass of MJE. Finally, a conjugate gradient energy minimization of full protein is performed until the root-mean-square (rms) gradient energy is lower than 0.001 kcal $mol^{-1}$. All calculations mentioned above are accomplished by using Dicover 3 software [18]. In this step, quality of the initial model is improved. During the optimization procedure, the structure is checked by Profile-3D and ProStat. The Profile-3D tests the validity of hypothetical protein structures by measuring the compatibility of the hypothetical structure with its own amino acid sequence [19,20]. The ProStat module of InsightII identifies and lists the number of instances where structural features differ significantly from average values calculated from known proteins.

### 2.2. Binding site analysis

The binding site module is a suite of programs in InsigtII for identifying and characterizing protein active sites, and multiple sequence alignments [21]. In this study, ActiveSite-Search is used to identify protein active sites and binding sites by

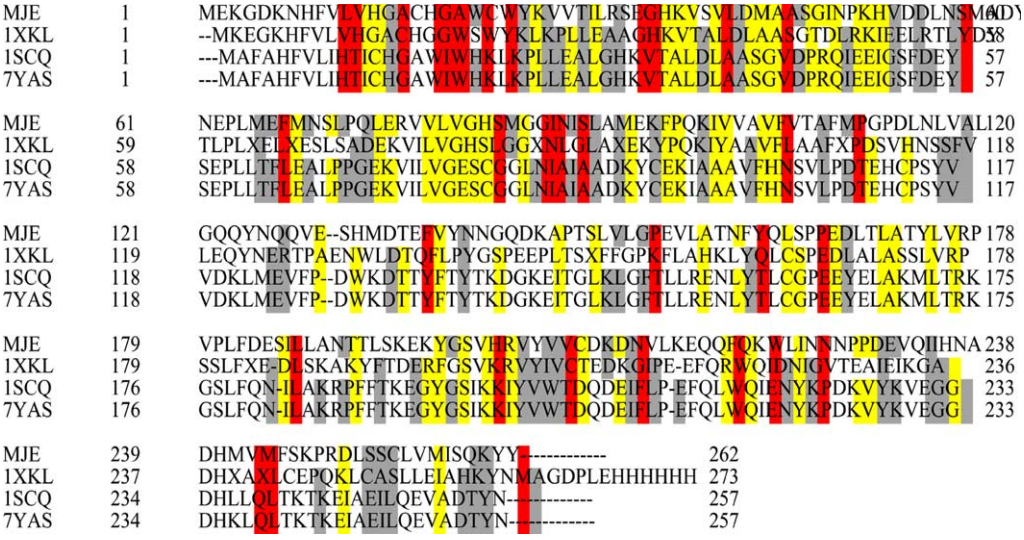


Fig. 1. Multiple sequence alignment of MJE with SABP2 (PDB code 1XKL), hydroxynitrile lyases from *Hevea brasiliensis* (PDB code 1SCQ), hydroxynitrile lyases from *Hevea brasiliensis* (PDB code 7yas). Red boxes show identical residues, yellow boxes show chemically similar residues, and gray boxes show semiconserved sunstitutions (for interpretation of the reference to colour in this legend, the reader is referred to the web version of this article).

locating cavities in MJE structures. When the search is completed, the largest site is automatically displayed on the structure other two sites are also obtained. The results can be used to guide the protein–ligand docking experiment.

### 2.3. Docking study

Molecular docking can fit molecules together in a favorable conformation to form a complex system. The structural information from the theoretically modeled complex may help us to clarify the catalytic mechanism of enzyme. The 3D structures of MeJA and phenylmethanesulfonyl fluoride are built with Builder program. The advanced docking program Affinity is adopted to perform the automated molecular docking [22]. The potential of complex is assigned by using CVFF force field. Nonbonding interactions are used for cell multiple approach. To account for the solvent effect, the centered enzyme–ligand complexes are solvated in a sphere of TIP3P water molecules with radius 10 Å. The whole complex structure is further refined by energy minimization with 1000 steps. This provides 10 structures from SA docking, and their generated conformations are clustered according to RMS deviation. The global structure with lowest energy is chosen for computing intermolecular binding energies. In general a higher Ludi score represents a higher affinity and stronger binding of a ligand to the receptor. Thus, for the complex structure, the Ludi program is used to character the affinity and the binding preference of a ligand to the receptor.

## 3. Result and discussion

### 3.1. Homology modeling of MJE

Three reference proteins, SABP2 (PDB code 1XKL) [14,23], hydroxynitrile lyases from Hevea brasiliensis (PDB code 1SCQ) [24], and hydroxynitrile lyases from Hevea brasiliensis (PDB code 7yas) [25], are used to model the structure of MJE. The homology scores comparing to target protein are 45, 36, and 36%, respectively, (see Fig. 1). As all the aligned protein proteins belong to the extremely divergent family of α/β-hydrolase fold proteins, it could be assumed that MJE is a member of this protein family [1]. Moreover, it should be noted that the sequence of amino acids determines the tertiary structure of a protein, as proposed by Christian Anfinsen [27]. On one hand, high level of sequence can guarantee more accurate alignment between the target sequence and template structure. On the other hand, MJE and hydroxynitrile lyases including 1SCQ and 7yas, which catalyze the cleavage of cyanohydrins to hydrocyanic acid plus the corresponding aldehyde or ketone, differ drastically in substrate specificity. So the most similar reference protein 1XKL is chosen as the template for modeling MJE. Then, the backbone coordinates of the residues in MJE are generated with the InsightII/Homology module. The structurally conserved regions (SCRs) are determined by multiple sequence alignment, which is based on the Needleman and Wunsch Algorithm [28]. The LOOPs between SCRs are more variable

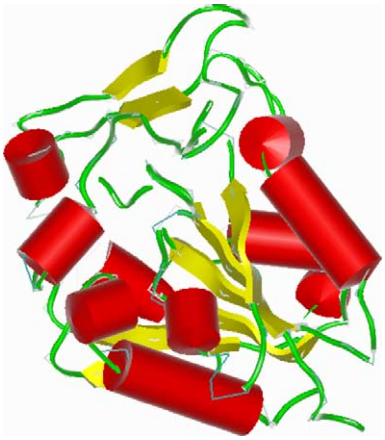

Fig. 2. The final 3D structure of MJE. The structure is obtained by energy minimizing an average conformation over the last 350 ps of MD simulation. The α-helix is represented in red and the β-sheet in the yellow (for interpretation of the references to colour in this figure legend, the reader is referred to the web version of this article).

in the conformation among the reference protein. The loop searching algorithm is used to construct the structure of LOOPs. All the side chains of model protein are set by rotamers and the structural optimization is preceded by using molecule mechanics and molecular dynamics methods. The final structure of MJE is presented in Fig. 2. The stability of the 3D model of MJE is refined by performing MD simulations. Fig. 3 displays potential energy of energy of the simulated system during the 350 ps of molecular dynamics. As seen from Fig. 3, the potential energy remains constant after 50 ps simulated time of molecular dynamics, which indicates that the 3D model of MJE is structurally stable after 50 ps MD time. Of these, the conformation with the lowest energy is chosen and the 3D structure is superimposed with 1XKL. Their root mean square deviation (RMSD) value was 0.58 Å. So the conformation with the lowest energy is used to evaluate. The homology model is very similar to the structure 1XKL. The overall secondary and tertiary structures are very similar for the two proteins. This also includes the loops adjacent to the active site. It is shown that the enzyme can be divided into two domains. The core domain contains a central six-stranded

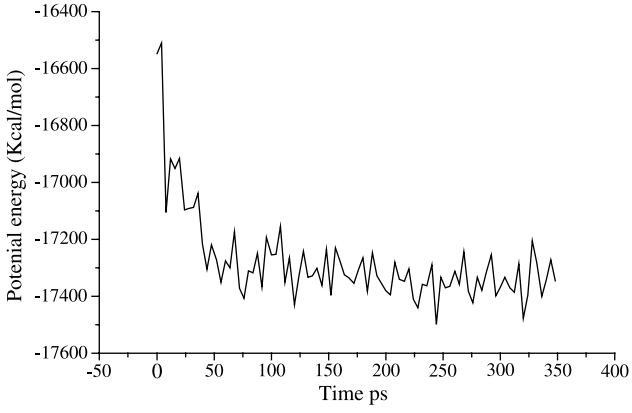


Fig. 3. The variation of total energy during the 350 ps of MD on the MJE. The total energy is averaged over 50 ps interval.

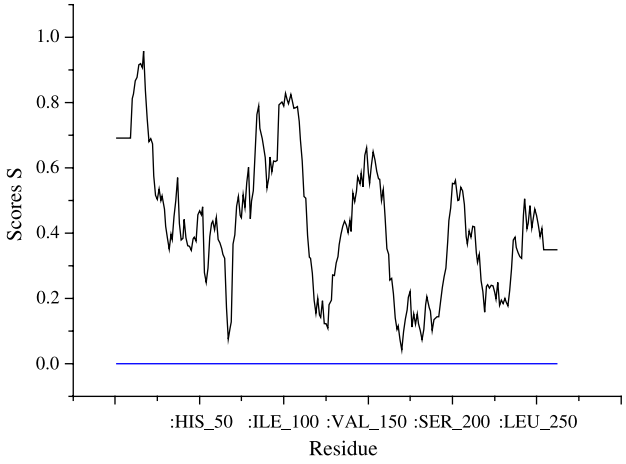


Fig. 4. 3D profiles of verified results of MJE model, residues with positive S are reasonably folded.

parallel β-sheet (named β1–β6) that is flanked on the both sides by six helices (αA–αF). The cap (or lid) domain contains a three-stranded antiparallel β-sheet ($\beta4_1$–$\beta4_3$) and three helices ($\alpha D_1$–$\alpha D_3$). The secondary structure elements are given with the same names as those in the structure of SABP2 [14,23].

The structure shown by Fig. 2 is checked by Profile-3D. The overall self-compatibility score for this protein is 104.13, which is higher than the lower score 53.59 and close to the top score 119.09 (Fig. 4). This means that the structure model of MJE is reasonable at the present level of theory. The ProStat is used to calculate the percent of backbone $\phi$–$\varphi$ angles within the allowed Ramachandran region. The result is that 80.8% of the $\phi$–$\varphi$ angles is in the MJE model. For the structure of SABP2, the percent of backbone $\phi$–$\varphi$ angles is 83.9%. Our calculated result implies that the modeling structure of MJE is reasonable. The ProStat is also used to identify and list the number of instances where structural features differ significantly from average values in known proteins, and there is not the case appeared that the bond lengths and the bond angles are different significantly. Using these geometric criteria, our MJE model is consistent with the structure of SABP2 (PDB code 1XKL) (Fig. 5).

Fig. 5. C α trace of MJE (represented by purple) and 1XKL (represented by blue colour) (for interpretation of the references to colour in this figure legend, the reader is referred to the web version of this article).

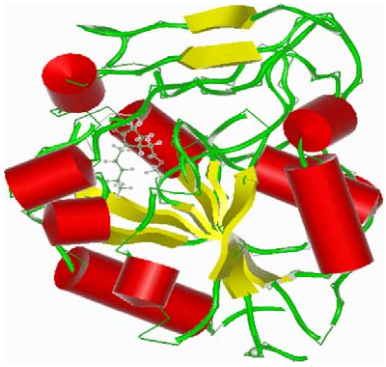

Fig. 6. A stereo picture of the 3D structure of the complex MJE–MeJA.

### 3.2. Identification of MeJA binding region in MJE

In order to simulate the interaction between MJE and MeJA, the MeJA-binding pocket was defined as a subset that contains residues in which any atoms were within 7.0 Å from MeJA. The 3D-structure of the complex MJE-MJA is displayed in Fig. 6. The binding pocket has the residues of Thr107, His240, Leu214, Asp211, Tyr124, Phe160, His82, Asp239, Gln220, Val106, Asn212, Val213, Ser83 and Ala108. As further support of this assumption, MJE shows the highly conserved amino acid residues forming the catalytic triad-nucheophile acid, represented by serine at position 83, aspartic acid at position 211, and histidine at position 240 [1,14]. The catalytic nucleophile Ser83 is located in the sharp turn (the Nucleophile elbow) between strand β3 and helix αC of the core domain, with a strained main-chain conformation. The second member of the triad, His240, is located in the loop connecting strand β6 and helix αF, whereas the third member of the triad, Asp211, is located in the loop connecting strand β5 and helix αE. The binding site of MJE is located at the C-terminal end of the parallel β-sheet in the core domain (Fig. 2). The cap domain, especially strands $\beta4_2$, $\beta4_3$ and $\alpha D_2$, $\alpha D_3$, covers the exposed side of the binding site (Fig. 2). From the alignment results, it is known that the residues of Asp211, His240, and Ser83 are conserved in four enzymes, and this means that three residues are important for the enzyme catalysis. These residues are strictly conserved among MJE and several closely related members of this superfamily [1,14,24,25]. As mention above, the largest site which contains Ser83, Asp211, and His240, is chosen as the binding site to dock the ligand.

### 3.3. Docking study

It is reported that the MJE is solely responsible for MeJA-cleaving activity [1], and it is important for us to investigate the binding mode of MeJA with MJE in the active site. As is well known, phenylmethanesulfonyl fluoride is serine hydrolases' inhibitor [13]. In order to investigate the inhibition mechanism and design a novel specific inhibitor for MJE, the docking studying of MJE with phenylmethanesulfonyl fluoride is also performed.

The structures of MeJA, and phenylmethanesulfonyl fluoride are built and optimized by the InsightII/Builder

program. The protein/ligand structures are analyzed by using Ludi method. The results show that the global structure with lowest energy has higher Ludi score, and it is chosen for computing intermolecular binding energies.

### 3.4. Docking of the ligand into the active site

It was reported that MJE possessed a conserved α/β hydrolase superfamily similar to that of SABP2 [1,14,15]. The MeJA–enzyme complex is developed by affinity module and the probable binding 3D conformation of MeJA–enzyme complex is shown by Fig. 6. Seen from Fig. 6, we know that MeJA is bound in the active-site pocket of the enzyme, where it is completely shield by the solvent and shows intimate polar and van der Waals contacts with the enzyme. The enzyme has a classic α/β fold composed of a central, parallel or mixed β sheet surrounded by α helices: the catalytic residues always constitute a highly conserved triad: a nucleophile (Ser83) positioned after strand β5, an Asp211, and His240 [14,26]. The nucleophile residue is always located in a very sharp turn, called the 'nucleophile elbow', where it can be easily approached by the substrate-MeJA. The nucleophile elbow is identified by the sequence Gly-His-Ser83-Met-Gly (Gly as small residue, Ser83 as nucleophic [26]). The tightness of this strand–turn–helix motif induces the nucleophilic amino acid residue to adopt energetically unfavorable main chain torsion angles and imposes steric restrictions on residues located in its proximity [14,26].

Hydrogen bonds play an important role for structure and function of biological molecules, especially for the enzyme catalysis. The hydrogen bonds presented in the complex are listed in Table 1 and Fig. 7. The side chain NH of Leu214 forms one hydrogen bond with cyclopentenone group of MeJA. The two hydrogen bonds are formed between the side chain OH of Thr107 and the main chain NH of Ser83 with carboxyl group of MeJA.

In addition, the Ser83 hydroxyl is not hydrogen-bonded to the second member His240 residue, and the hydrogen-bonding network among the catalytic triad residues is not formed in this complex. In a mechanistic proposition, residues of the catalytic triad act as a general acid/base, involving deprotonation of OH-Ser83 by His240 and concomitant abstraction of a proton from the substrate hydroxyl by Ser83. During MeJA-cleaving, His240-Asp211 pair undergoes a protonation/deprotonation during a catalytic cycle [1,14]. It is reported that a role for the active site residue Asp211, in which the positive charge was proposed to stabilize the complementary negative charge, was also responsible for correctly positioning the substrate [14,26].

Table 1
The hydrogen bonds between MeJA and binding pocket residues of MJE

| MJE | | MeJA atom | Distance (Å) | Angle |
|---|---|---|---|---|
| Residue | Atom | | | |
| Ser83 | NH | O11 | 2.19 | 135.95 |
| Thr107 | OH | O6 | 1.48 | 167.76 |
| Leu214 | NH | O | 2.21 | 134.34 |

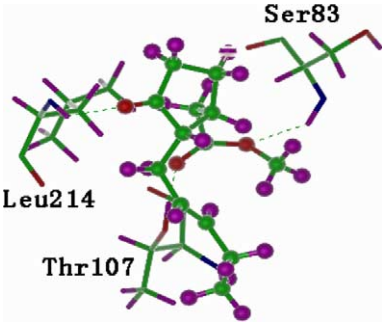


Fig. 7. The hydrogen bonding interactions of MeJA–MJE.

It is reported that the only changed residue is the catalytic Ser83, by assuming a different torsion angle, and the side chain of this residue can become hydrogen bonded to that of His240, completing the catalytic triad [14]. The structural information of the MeJA–MJE complex shows that the active site pocket of MJE is less than that of SABP2's, but it can accommodate the substrate: MeJA. MeJA is located in a highly hydrophobic environment, surrounded by side chains from the core and the cap domains. Particularly, the side chains of Gln123, His131, Phe136, Leu149, and Leu181 in the cap domain shield the MeJA molecule from the solvent. Moreover, because the active site is completely shielded from the solvent, the enzyme is expected to undergo an open-closed transition to allow substrate binding and product release.

To determine the key residues in binding pocket of the model, the interaction energies of the substrate with each individual amino acid in the enzyme are calculated. Table 2 gives the interaction energies including the total, van der Waals and electrostatic ones with the total energy lower than $-1.00$ kcal mol$^{-1}$ for all residues in MJE. The total energies, van der Waals and electrostatic energies are $-51.68$, $-42.84$, $-8.84$ kcal mol$^{-1}$, respectively. This means that the interaction is mainly attractive interaction. Thus, we can conclude that in this case van der Waals is important for determining the binding orientations. Through interaction analysis, we know that Thr107, His240, Leu214, Asp211, Tyr124, Phe160, His82,

Table 2
The total energy $E_{total}$, van-der-Waal energy $E_{vdw}$ and electrostatic energy $E_{ele}$ between MeJA and individual residues ($E_{total} < -1.00$ kcal mol$^{-1}$ listed in energy rank order)

| Residues | $E_{vdw}$ (kcal mol$^{-1}$) | $E_{ele}$ (kcal mol$^{-1}$) | $E_{total}$ (kcal mol$^{-1}$) |
|---|---|---|---|
| Thr107 | −1.12 | −5.61 | −6.72 |
| His240 | −3.86 | −2.02 | −5.88 |
| Leu214 | −4.64 | −0.64 | −5.27 |
| Asp211 | −2.04 | −2.82 | −4.86 |
| Tyr124 | −3.32 | 0.02 | −3.21 |
| Phe160 | −3.66 | 0.74 | −2.92 |
| His82 | −2.68 | 0.71 | −1.97 |
| Asp239 | −1.23 | −0.51 | −1.74 |
| Gln220 | −0.92 | −0.79 | −1.71 |
| Val106 | −1.74 | 0.05 | −1.69 |
| Asn212 | −1.02 | −0.66 | −1.68 |
| Val213 | −0.55 | −1.09 | −1.64 |
| Ser83 | −1.01 | −0.38 | −1.39 |
| Ala108 | −2.54 | 1.48 | −1.06 |

Table 3
The hydrogen bonds between phenylmethanesulfonyl fluoride and binding pocket residues of MJE

| MJE | | Phenylmethanesulfonyl fluoride | | Distance (Å) | Angle |
|---|---|---|---|---|---|
| Residue | Atom | | Atom | | |
| His82 | NH | Sulfonyl | O | 2.48 | 123.74 |
| Ser83 | NH | Sulfonyl | F | 2.15 | 153.03 |
| His240 | NH | Sulfonyl | S | 3.26 | NA |
| His240 | NH | | | 2.92 | NA |

Asp239, Gln220, Val106, Asn212, Val213, Ser83 are important anchoring residues for MJE. It reported that Ser83, Asp211 and His240 are important anchoring residues [1], and this conclusion is identical of our result. Thr107, Leu214 may be an important residue because they form a hydrogen bond with MJE. For the hydrophobic residues of Val106, Ala108, Phe160, Val213, and Leu214, the interaction energies with MeJA are mainly contributed by van der Waals interaction. Especially, the van der Waals and electrocutions energies between Ser83 and MeJA are $-1.01$ and $-0.38$ kcal mol$^{-1}$, respectively. We think that the residue of Ser83 of the catalytic triad is essential for MJE' esterase activity, which agrees with the results that was inferred by experimental study [1,14]. On the other hand, the energy information given by Table 2 may comply with the candidate sites for further experimental studies of site-directed mutagenesis (Table 3).

### 3.5. Docking of the inhibitor into the active site

To understand the interaction between MJE and phenylmethanesulfonyl fluoride, the MJE–phenylmethanesulfonyl fluoride (M–p) is generated using the InsightII/Affinity module. Phenylmethanesulfonyl fluoride also locates in the center of the active site (Fig. 8), and there are four hydrogen bonds between MJE and phenylmethanesulfonyl fluoride (Table 4 and Fig. 9). The two hydrogen bonds are formed between the side chain NH of His240 and Sulfonyl group of phenylmethanesulfonyl fluoride and the main chain NH of Ser83 forms one hydrogen bond with fluoride group of phenylmethanesulfonyl fluoride. The imidazoles's NH of His82 forms a tight hydrogen bond to sulfonyl group. These hydrogen bonding interactions may enhance the stability of M–p complex. Among these hydrogen bonding interactions, we think that His240, Ser83, and His82 are the main contributors to the M–p complex because they form hydrogen bonds with MJE. In particular, Ser83 is bound to phenylmethanesulfonyl fluoride and cannot act as the necleophile. His240 forms two H-bonds with phenylmethanesulfonyl fluoride, and the imidazole's group is tightly bound to inhibitor, therefore destroying the deprotonation of OH-Ser83 by His240.

Table 4
The total energy $E_{total}$, van-der-Waal energy $E_{vdw}$ and electrostatic energy $E_{ele}$ between phenylmethanesulfonyl fluoride and individual residues ($E_{total} < -0.62$ kcal mol$^{-1}$ listed in energy rank order)

| Residues | $E_{vdw}$ (kcal mol$^{-1}$) | $E_{ele}$ (kcal mol$^{-1}$) | $E_{total}$ (kcal mol$^{-1}$) |
|---|---|---|---|
| His240 | −3.00 | −1.64 | −4.64 |
| His82 | −3.46 | −1.08 | −4.54 |
| Tyr124 | −2.62 | −0.38 | −3.00 |
| Phe109 | −2.52 | −0.06 | −2.58 |
| Phe160 | −2.16 | −0.32 | −2.48 |
| Thr107 | −1.86 | −0.61 | −2.47 |
| Ser83 | 0.52 | −2.78 | −2.26 |
| Leu214 | −2.33 | 0.08 | −2.25 |
| Ala108 | −1.96 | −0.19 | −2.15 |
| Met84 | −1.82 | 0.17 | −1.65 |
| Val213 | −1.04 | 0.33 | −0.71 |
| Asp211 | −0.43 | −0.19 | −0.62 |

To determine the key residues that comprise the active site of the model, the interaction energies of the ligand with each of the residues in the active of MJE are calculated. Table 4 gives these interaction energies including the total, van der Waal and electrostatic energies, for all residues with a total energy lower than $-0.61$ kcal mol$^{-1}$ in the M–p complex. From Table 5 we can see that the M–p complex has favorable total interaction energy of $-35.53$ kcal mol$^{-1}$, the van der Waals and electrostatic energies are $-29.78$ and $-5.75$ kcal mol$^{-1}$, respectively. It means that the interaction is mainly attractive interaction. From this result, we suggest that His240, His82, Trp124, Phe109, Phe160, Thr107, Ser83, Leu214, Ala108, Met84, Val213, and Asp211 are important anchoring residues for MJE and are main contributors to the inhibitor interaction. It should be noted that Ser83 is an important anchoring residue [13], and this conclusion is identical with our result. The total interaction energy between MJE and His240 is $-4.64$ kcal mol$^{-1}$ in which the primary interaction energy is

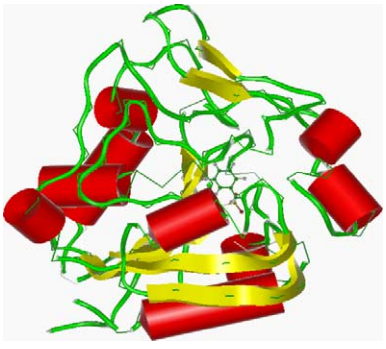

Fig. 8. The stereo picture of the 3D structure of the complex MJE–phenylmethanesulfonyl fluoride.

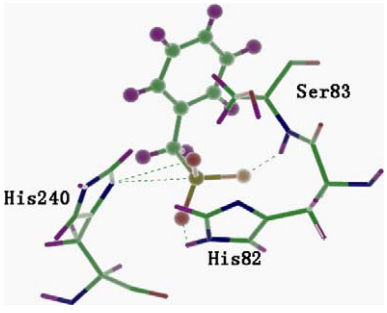


Fig. 9. The hydrogen bonding interactions of MJE–phenylmethanesulfonyl fluoride.

Table 5
The calculated energies of MeJA and inhibitor phenylmethanesulfonyl fluoride tested for MJE binding

| Ligand | Total energy | $E_{vdw}$ (kcal mol$^{-1}$) | $E_{ele}$ (kcal mol$^{-1}$) | Ludi score |
|---|---|---|---|---|
| MeJA | −51.68 | −42.84 | −8.84 | 355 |
| Phenyl-methane-sulfonyl fluoride | −35.53 | −29.78 | −5.75 | 399 |

van der Waals interaction one (−3.00 kcal mol$^{-1}$). It is well known that Ser is weak acid and there is the proton-transfer reaction between Ser83 and His240. In M–p complex, His240 bound tightly to phenylmethanesulfonyl fluoride and the interaction energy between His240 and inhibitor is the lowest. Thus, on one hand, the proton transfer from serine residue to histidine may be break down, and the acidity of serine decreases. Low acidity of the base of catalytic triad is often associated with a low enzymatic activity. On the other hand, histidine bound tightly to the inhibitor and it is difficult to be taken out. Therefore, this substitution may cause spatial obstruction and prevent the substrate from docking into MJE. The residues of His82, Trp124, Phe109, Phe160, Thr107, Leu214, Ala108, Met84, Val213, and Asp211 have the similar behavior as His240 and the interaction energies of these residues with MJE are mainly contributed by van der Waals interaction. But, for the residue of Ser83, the interaction energies of this residue with MJE are mainly contributed by electronic interaction. As shown in Tables 4 and 5, these results can serve as a guide for the selection of candidate sites for further experimental studies of site-directed mutagenesis.

In order to compare with the binding affinity of a ligand to the receptor, the Ludi program is used and the results are listed in Table 5. From Table 5, we can see that the total interaction energy between MeJA–MJE is lower than that of phenyl-methanesulfonyl fluoride–MJE. It may come from more atoms in MeJA. However, Ludi score for phenylmethanesulfonyl fluoride–MJE (399) is higher than MeJA–MJE (355). This indicates that phenylmethanesulfonyl fluoride has higher affinity and stronger binding than MeJA. This result is consistent with the experimental facts [13].

## 4. Conclusion

MJE is a highly conserved α/β superfamily ester enzyme implicated in jasmonate signaling. Up to now, the 3D structure of MJE is not identified. In this paper, we have developed a three-dimensional model of MJE by Insight-II/Homology module. After energy minimization and molecular dynamics simulations, the refined model structure is obtained. The final refine model is assessed by Profile-3D and ProStat, and the results show that this model is reliable, and the general 3D organization of MJE is a typical α/β hydrolase family. The docking studying of the complex MJE–MeJA shows that the Ser83 as nucleophile residue is important for MJE catalysis. In addition, Thr107 and Leu214 have been identified for the model and they are involved in strong hydrogen bonding interaction with substrate. Val106, Ala108, Phe160, and Val213 also appear as important hydrophobic binding-site residues for the model. These residues are prime targets for site-directed mutagenesis experiments and as candidates for structure–function relationships. It is notable that it is an irreversible inhibitor of serine hydrolases, which is consistent with the experimental facts. His240 and His82 are involved in inhibitor binding and they may play an important role in inhibition. In addition, as well as others in Tables 2 and 4, these residues are suggested as candidates for further experimental studies of structure-function relationships.

## Acknowledgements

This work was supported by the National Science Foundation of China (20333050, 20073014), Doctor Foundation by the Ministry of Education, Foundation for University Key Teacher by the Ministry of Education, Key subject of Science and Technology by the Ministry of Education of China, and Key subject of Science and Technology by Jilin Province.

## References

[1] Stuhlfelder C, Mueller MJ, Warzecha H. Eur J Biochem 2004;271:2976.
[2] Preston CA, Lewandowski C, Enyedi AJ, Baldwin IT. Planta 1999;209:87.
[3] Howe GA. Proc Natl Acad Sci 2001;98:12317.
[4] Li L, Li C, Lee GI, Howe GA. Proc Natl Acad Sci 2002;99:6416.
[5] Green TR, Ryan CA. Science 1972;175:776.
[6] Farmer EF, Ryan CA. Proc Natl Acad Sci 1990;87:7713.
[7] Seo HS, Song JT, Cheong J-J, Lee Y-H, Lee Y-W, Hwang I, et al. Proc Natl Acad Sci 2001;98:4788.
[8] Stintzi A, Weber H, Reymond P, Browse J, Farmer FE. Proc Natl Acad Sci 2001;98:12837.
[9] Thomma BPHJ, Eggermont K, Penninckx IAMI, Mauch-Mani B, Vogesang R, Cammue BPAC, et al. Proc Natl Acad Sci 1998;95:15107.
[10] Casaretto JA, Zuniga GE, Corcuera LJ. J Plant Physiol 2004;161:389.
[11] Cipollini D, Enright S, Traw MB, Bercelson J. Mol Ecol 2004;13:1643.
[12] Kachroo A, Lapchyk L, Fukushige H, Hildebrand D, Klessig D. Plant Cell 2003;15:2952.
[13] Stuhlfelder C, Lottspeich F, Mueller MJ. Phytochemistry 2002;60:233.
[14] Forouhar F, Yan Y, Kumar D, Chen Y, Fridman E, Park SW, et al. Proc Natl Acad Sci 2005;102:1773.
[15] InsightII, version 2000. San Diego: Accelrys, Inc.; 2000.
[16] Homology user guide, Accelrys, Inc., San Diego, USA; 1999.
[17] Altschul SF, Glisli W, Miller W, Mayer EW, Lipman DJ. J Mol Biol 1990;215:403.
[18] Discover3 user guide, Accelrys, Inc., San Diego, USA; 1999.
[19] Profile-3D user guide, Accelrys, Inc., San Diego, USA; 1999.
[20] Luthy R, Bowie JU, Eisenberg D. Nature 1992;356:82.
[21] Binding site analysis user guide, Accelrys, Inc., San Diego, USA; 1999.
[22] Affinity user guide, Accelrys, Inc., San Diego, USA; 1999.
[23] Kumar D, Klessig DF. Proc Natl Acad Sci 2003;00:16101.
[24] Hasslacher M, Kratky C, Grieng H, Schwab H, Kohlwein SD. Struct Funct Genet 1997;27:438.
[25] Gruber K, Gartler G, Krammers B, Schwab H, Kratky C. J Biol Chem 2004;279:20501.
[26] Nardini M, Dijkstra B. Curr Opin Struct Biol 1999;9:732.
[27] Anfinsen CB, Redfield RR, Choate WL, Page J, Carroll WR. J Biol Chem 1954;207:201.
[28] Needleman SB, Wunch CD. J Mol Biol 1970;48:443.